# TIME-RESOLVED TEMPERATURE MAPPING SYSTEM FOR THE APS DEFLECTING CAVITIES*

Y. Yang †‖, P. Dhakal#, J. Fuerst, J. Holzbauer, J. Kaluzny, J. Mammosser#,
A. Nassiri, H. Wang#, G. Wu, Argonne National Laboratory, Argonne, IL 60439, USA
#Thomas Jefferson National Accelerator Facility, Newport News, VA 23606, USA
‖Tsinghua University, Beijing 100084, China

*Abstract*

Time-resolved temperature mapping of a superconducting cavity can give valuable information on the limiting process of the cavity performance. A fast temperature mapping system has been developed at Argonne National Laboratory (ANL) for a superconducting deflecting cavity test. The time resolution of the temperature mapping could be up to 50 $\mu$s. Not only the spatial distribution of surface heating but also the thermodynamics can be recorded, which helps to understand the limitation mechanism. This new temperature mapping system has helped us to understand the rf performance limitations during the cavity vertical tests. Based on the findings from the temperature mapping, proper cavity treatment has been applied and the cavity performances have been improved.

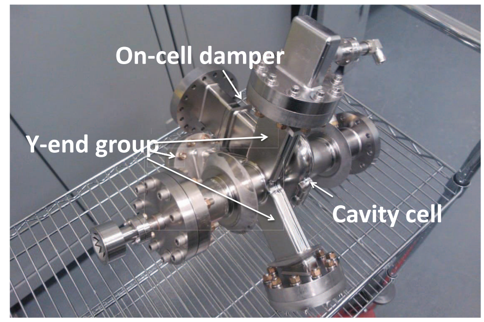


Figure 1: The APS superconducting deflecting cavity during assembling in a clean room. The cavity has a Y-end group on the beam pipe and a on-cell waveguide damper.

## INTRODUCTION

The Advanced Photon Source (APS) at Argonne National Lab (ANL) has considered using the superconducting deflection technique to generate x-rays on the order of 2 ps or less [1]. A single-cell cavity design has been chosen as the baseline design and four superconducting deflecting cavities have been fabricated, as shown in Fig. 1. The cavity is a single squashed-cell cavity with an on-cell waveguide damper and a Y-end group on the beam pipe [2]. To provide sufficient deflecting modulation to the beam, a single-cavity deflecting voltage needs to reach 0.5 MV, which corresponds to a peak surface magnetic field of 106 mT. To accomplish this challenging goal, it is very important to understand the cavity performance limitations. Generally speaking, a number of processes, such as multipacting, field-emission, Q-slope, and thermal quench, might limit the superconducting cavity performance. All of these processes will eventually generate heat on the cavity wall. Temperature mapping is presently one of the most effective tools to gain insight into the cavity limitations.

Most conventional temperature mapping systems work for L-band accelerators [3][4]. Hundreds of sensors are required to cover the cavity surface. However, the sampling rate is limited to a few Hz, which is not fast enough to get a resolved signal. The APS deflecting cavity operates at 2815 MHz. The cavity size is much more compact compared to the L-band cavity, thus a fewer number of sensors are needed to cover the high magnetic field surface. A new time-resolved temperature mapping system has been developed for the APS deflecting cavity. It consists of 24 temperature sensors with a time resolution as high as 50 $\mu$s. A number of cavity tests made using this system have helped us understand cavity performance limitations. Compared to conventional temperature mapping, time-resolved temperature signals are much superior in classifying the limitations in terms of thermal dynamics. These findings from temperature mapping have led us to improve the cavity performance with the following treatment.

## SENSOR MOUNTING AND DATA ACQUISITION

We used sensors made from Allen-Bradley carbon resistors. This resistor has a high thermal sensitivity of 10Ω/mK around 2 K. To thermally isolate the sensor from the helium bath, the resistor was enclosed in a G-10 container filled with epoxy. In order to make good thermal contact and provide electrical isolation to the cavity surface, the top surface of the resistor was ground away until the carbon was exposed and then a thin layer of a GE-varnish, toluene and alcohol mixture was applied.

The APS deflecting cavity operates at dipole mode, and the highest surface magnetic field region is the iris between the cavity cell and the Y-end group. The sensors were mounted around the cavity based on the surface magnetic field distribution, as shown in Fig. 2. Proper mounting techniques were developed. A cryogenic cable tie was applied as a band to mount the sensors around the iris. Two semi-circle bands made of cryogenic fiberglass weres used to attach the sensors on the cavity cell. Apiezon N grease

* Work supported by the U.S. Department of Energy, Office of Science, under Contract No. DE-AC02-06CH11357
† yaweiyang@aps.anl.gov

is applied to all the sensor contacts to ensure good thermal contact with the cavity.

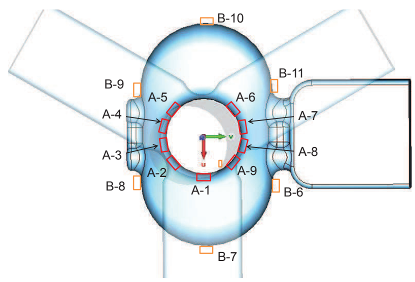


Figure 2: Sensor layout around the cell and the iris looking from the Y-end group side. The iris on the other side has similar sensors around the iris.

The data acquisition is based on a National Instrument data acquisition (DAQ) device. However, direct connection of the sensor to the DAQ will result in excessive current to the sensor. A proper circuit is designed to excite the sensors with a 15-$\mu A$ current. As shown in Fig. 3 , the resistance values of the sensors are measured in terms of the voltage drop across the resistor. The cavity field level can be measured in terms of the output voltage of the cavity transmitted power crystal detector. All the data is processed and recorded by a LabVIEW program.

The software has three operation modes: calibration mode, continuous measurement mode, and pulse measurement mode. The calibration mode records how the resistance of different sensors changes with the helium gas pressure reading. Those correlations are used to calculate the temperature rise during the measurement. The calibration mode operates during the helium-bath cooling from 4 K to 2 K. The sampling rate is only 0.5 Hz, but the accuracy is better than 0.3 mK. During the cavity test, the software usually operates in continuous measurement mode. It quickly records the resistance values of different sensors. Then the temperature is calculated using the calibrated correlations. The sampling rate of continuous mode is 300 Hz with an accuracy of 2 mK, which is fast and accurate enough to obtain time-resolved heating. The pulse mode records the sensor reading with highest possible resolution up to 50 $\mu$s. However, the accuracy is limited to about 10 mK and the measurement only lasts for 2 seconds. This mode is designed to give the highest time-resolution.

## CAVITY VERTICAL TEST WITH TIME-RESOLVED TEMPERATURE MAPPING

Eight cavity vertical tests have been performed with this temperature mapping system, and it has helped to identify the limitations of the cavity performances. With the help of this system, a number of defect mechanisms have been identified that have lead us to find appropriate treatment techniques to eliminate the obstacles and improve the cavity performance.

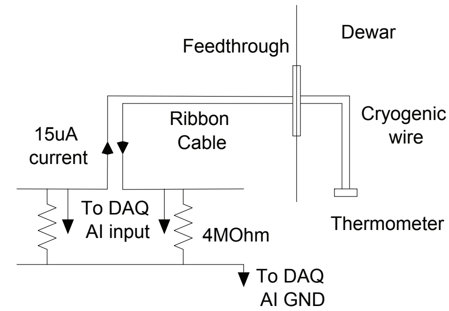


Figure 3: Schematic of the measurement circuit. A 15 $\mu$A current is used to excite the thermometer, and the voltage drop across the resistor is used to measure the resistance value.

### *Multipacting*

The thermodynamics of multipacting (MP) on the cavity wall can be obtained using this system. It can be identified as an abrupt pulse heating when the field level reaches a barrier and then has a small and abrupt drop. An example is given in Fig. 4. Sensors A-3 and A-8 detected pulse heating signals during the vertical test when the cavity surface peak magnetic field first approached 85 mT.

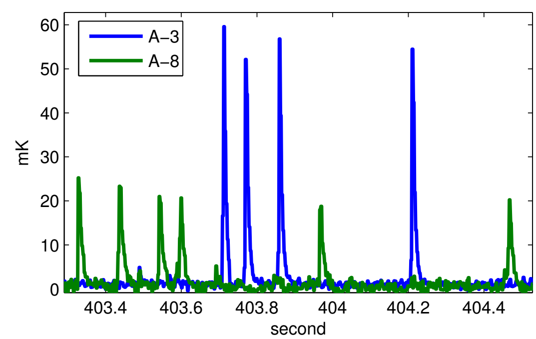


Figure 4: A soft MP barrier occurred at the A-3 and A-8 sensors when the maximum surface M-field approached 85 mT. Pulse heating can be detected when MP occurs

It can be seen that multipacting induced pulsed heatings at A-3 and A-8. They did not happen at the same time. On the other hand, both the A-3 and A-8 sensors were located at high magnetic field regions. The multipacting at either point is likely one-point multipacting.

All the multipacting found in the cavity tests turned out to be soft. The thermodynamic during multipacting processing was also obtained. The processing lasted from tens of seconds to several minutes. After that, the processing subsided and the Q gradually returned to normal. A continuous but not stable heating signal could be detected by time-resolved temperature mapping during the processing. Figure 5 shows an example of temperature signals during multipacting processing. The pulse heating signals became a continuous heating signal when the processing started. The processing happened at two points: the


ISBN 978-3-95450-138-0

A-3 sensor location and the A-8 sensor location. An interesting phenomenon was that the processing at A-3 and A-8 took place alternately, which formed a rectangular-shaped temperature-rise signal. The processing gradually decayed as the temperature went down, and cavity Q gradually increased back to a normal level.

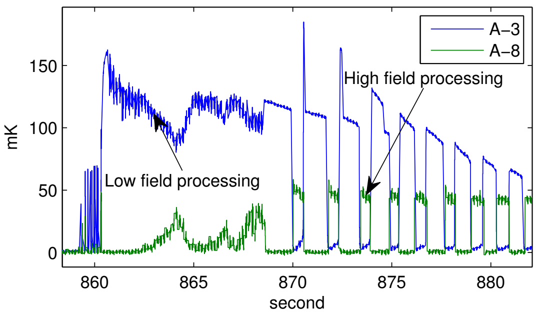


Figure 5: MP processing happened at A-3 and A-8 sensor when peak magnetic field approached 95 mT. The sudden "turn on" of the processing is shown with pulse heating changing into a continuous heating signal.

### *High-Field Q-Slope*

High-field Q-slope was found in one of the cavities starting at 70 mT. The temperature mapping showed the Y-end group iris had a strong heating signal all around the iris [5]. The time-resolved signal showed the heating magnitude was constant at a given cavity field level. After the cavity showed a Q-slope at high field, the temperature rose exponentially in the power law ranging from 10 to 16. Those findings were consistent with the finding of Q-slope with convectional temperature mapping.

### *Quench Detection*

Quench detection becomes more accurate with time-resolved temperature mapping. The thermodynamics of quench can be recorded. Figure 6 gives an example of quench. When quench happened, the A-3 sensor set at the location of the quench measured a pulse heating reading as soon as the cavity field dropped to zero. The pulse heating magnitude was very high (the highest reading was about 1.5K), which lasted about 50 ms. The sensors within 0,5 inch detected a small pulse reading of tens of mK. However, other hot spot temperatures would drop as the cavity quenched. The thermodynamics demonstrated by the time-resolved temperature mapping could help to determine the quench location with good accuracy.

## CAVITY PERFORMANCE IMPROVEMENT

Of the four fabricated deflecting cavities, two of them have been explored in detail with this temperature mapping system. It has successfully located the defect spots or

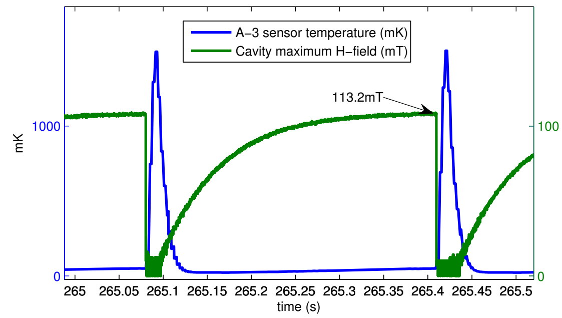


Figure 6: Quench pulse heating signal, the quench location temperature heating can go as high as 1.5K.

the heating area, and helped us to understand the performance limitations. Based on the findings from temperature mapping, the following treatments have helped to improve performance [6]. In one cavity, global heating was detected around the iris. A 40$\mu$m EP has helped to remove the Q-slope and improve the quench limit. In the other cavity, quench was detected at one spot on the cavity equator when the peak magnetic field approached 95 mT. A welding defect was found at the spot by optical inspection. The subsequent cosmetic E-beam welding smoothed the area and improved the gradient. Both of the cavities have reached design specifications.

## SUMMARY

We described a time-resolved temperature mapping system to characterize the performance limitations of the APS deflecting cavity. Time-resolved temperature signals can be used to gain further insight into these limitations. Detailed studies were performed in two deflecting cavities. Based on our findings, proper treatment was applied and cavity performance reached design criteria in both cavities.

## REFERENCES

[1] M. Borland, Physical Review Special Topics-Accelerators and Beams 8 (2005) 074001.

[2] A. Nassiri et al., "Status of the Short-Pulse X-Ray Project at the Advanced Photon Source," IPAC 2012, WEPPC038, p. 2292 (2012).

[3] A. Canabal et al., "Development of a temperature mapping system for 1.3-GHz 9-cell SRF cavities," PAC 2007, WEPMS031, p. 2406 (2007)

[4] G. Ciovati et al., "Temperature mapping system for single cell cavities," JLAB-TN-05-059, 2005.

[5] Y. Yang et al., "Electropolishing of the ANL deflecting cavity for the APS upgrade," SRF 2013, TUP055, to be published.

[6] J. Mammosser et al., "Fabrication and testing of defecting cavities for APS," SRF 2013, FRIOA03, to be published.